POLITECNICO DI TORINO
Repository ISTITUZIONALE

New high precision measurements of the cosmic charged particle rate beyond the Arctic Circle with the PolarquEEEst experiment

Original
New high precision measurements of the cosmic charged particle rate beyond the Arctic Circle with the PolarquEEEst experiment / Abbrescia, M.; Avanzini, C.; Arlandoo, M.; Balbi, G.; Baldini, L.; Ferroli, R. B.; Batignani, G.; Battaglieri, M.; Boi, S.; Cavazza, D.; Bossini, E.; Carnesecchi, F.; Cicalò, C.; Cifarelli, L.; Coccetti, F.; Coccia, E.; Corvaglia, A.; De Gruttola, D.; De Pasquale, S.; Fabbri, F.; Falchieri, D.; Flammini, A.; Galante, L.; Garbini, M.; Gemme, G.; Gnesi, I.; Gramstad, E.; Grazzi, S.; Håland, E. S.; Hatzifotiadou, D.; La Rocca, P.; Liu, Z.; Lombardo, L.; Mandaglio, G.; Margotti, A.; Maron, G.; Mazziotta, M. N.; Meneghini, S.; Millerjord, S. A.; Mulliri, A.; Nania, R.; Noferini, F.; Nozzoli, F.; Ould-Saada, F.; Palmonari, F.; Panareo, M.; Panetta, M. P.; Paoletti, R.; Parvis, M.; Pellegrino, C.; Perasso, L.; Pinazza, O.; Pinto, C.; Pisano, S.; Riggi, F.; Righini, G.; Ripoli, C.; Rizzi, M.; Sartorelli, G.; Scapparone, E.; Schioppa, M.; Scioli, G.; Scribano, A.; Selvi, M.; Serri, G.; Squarcia, S.; Taiuti, M.; Terreni, G.; Torromeo, G.; Travaglini, R.; Trifirò, A.; Trimarchi, M.; Veri, C.; Vistoli, C.; Votano, L.; Williams, M. C. S.; Zichichi, A.; Zuyeuski, R.. - In: THE EUROPEAN PHYSICAL JOURNAL. C, PARTICLES AND FIELDS. - ISSN 1434-6044. - STAMPA. - 80:7(2020), pp. 1-20. [10.1140/epjc/s10052-020-8213-2]
Published
DOI:10.1140/epjc/s10052-020-8213-2

Terms of use:

This article is made available under terms and conditions as specified in the corresponding bibliographic description in the repository

Publisher copyright
Springer postprint/Author's Accepted Manuscript

This version of the article has been accepted for publication, after peer review (when applicable) and is subject to Springer Nature's AM terms of use, but is not the Version of Record and does not reflect post-acceptance improvements, or any corrections. The Version of Record is available online at: http://dx.doi.org/10.1140/epjc/s10052-020-8213-2

(Article begins on next page)

Availability:
This version is available at: 11583/2841663 since: 2020-12-12T18:06:20Z

Publisher:
Springer Verlag

29 March 2024

Eur. Phys. J. C (2020) 80:665
https://doi.org/10.1140/epjc/s10052-020-8213-2

THE EUROPEAN PHYSICAL JOURNAL C

Regular Article - Experimental Physics

New high precision measurements of the cosmic charged particle rate beyond the Arctic Circle with the PolarquEEEst experiment

M. Abbrescia[1,2,a], C. Avanzini[3,4], M. Arlandoo[5], G. Balbi[6], L. Baldini[3,4,7], R. Baldini Ferroli[4,8], G. Batignani[3,4,7], M. Battaglieri[4,9,10], S. Boi[4,11,12], D. Cavazza[6], E. Bossini[13], F. Carnesecchi[4,6,14], C. Cicalò[4,12], L. Cifarelli[4,6,14], F. Coccetti[4], E. Coccia[4,15], A. Corvaglia[4,16], D. De Gruttola[17,18], S. De Pasquale[17,18], F. Fabbri[4,8], D. Falchieri[6], A. Flammini[6], L. Galante[4,19,20], M. Garbini[4,6], G. Gemme[9], I. Gnesi[4,21], E. Gramstad[5], S. Grazzi[4], E. S. Håland[5], D. Hatzifotiadou[6,13,4], P. La Rocca[4,22,23], Z. Liu[24], L. Lombardo[25], G. Mandaglio[4,23,26], A. Margotti[6], G. Maron[27], M. N. Mazziotta[2,b], S. Meneghini[6], S. A. Millerjord[5], A. Mulliri[11,12], R. Nania[6,4], F. Noferini[4,6,c], F. Nozzoli[28], F. Ould-Saada[5], F. Palmonari[4,6,14], M. Panareo[16,29], M. P. Panetta[4,16], R. Paoletti[3,30], M. Parvis[25], C. Pellegrino[4,27], F. Riggi[4,22,23], G. Righini[31], C. Ripoli[17,18], M. Rizzi[2], G. Sartorelli[4,6,14], E. Scapparone[4,6], M. Schioppa[21,32], G. Scioli[6,14], A. Scribano[30], M. Selvi[4,6], G. Serri[4,11,12], S. Squarcia[9,33], M. Taiuti[9,33], G. Terreni[3,4], G. Torromeo[6], R. Travaglini[6], A. Trifirò[4,23,26], M. Trimarchi[4,23,26], C. Veri[6], C. Vistoli[27], L. Votano[34], M. C. S. Williams[4], A. Zichichi[4,6,13,14], R. Zuyeuski[4]

[1] Dipartimento Interateneo di Fisica, Università di Bari, Bari, Italy
[2] INFN Sezione di Bari, Bari, Italy
[3] INFN Sezione di Pisa, Pisa, Italy
[4] Museo storico della Fisica e Centro studi e ricerche "E. Fermi", Roma, Italy
[5] Physics Department, Oslo University, Oslo, Norway
[6] INFN Sezione di Bologna, Bologna, Italy
[7] Dipartimento di Fisica, Università di Pisa, Pisa, Italy
[8] INFN, Laboratori Nazionali di Frascati, Frascati (RM), Italy
[9] INFN Sezione di Genova, Genova, Italy
[10] Thomas Jefferson National Accelerator Facility, Newport News, VA 23606, USA
[11] Dipartimento di Fisica, Università di Cagliari, Cagliari, Italy
[12] INFN Sezione di Cagliari, Cagliari, Italy
[13] CERN, Geneva, Switzerland
[14] Dipartimento di Fisica, Università di Bologna, Bologna, Italy
[15] Gran Sasso Science Institute, L'Aquila, Italy
[16] INFN Sezione di Lecce, Lecce, Italy
[17] Dipartimento di Fisica, Università di Salerno, Salerno, Italy
[18] INFN Gruppo Collegato di Salerno, Salerno, Italy
[19] Dipartimento di Scienze Applicate e Tecnologia, Politecnico di Torino, Torino, Italy
[20] INFN Sezione di Torino, Torino, Italy
[21] INFN Gruppo Collegato di Cosenza, Laboratori Nazionali di Frascati (RM), Frascati, Italy
[22] Dipartimento di Fisica e Astronomia, Università di Catania, Catania, Italy
[23] INFN Sezione di Catania, Catania, Italy
[24] ICSC World laboratory, Geneva, Switzerland
[25] Dipartimento di Elettronica e Telecomunicazioni, Politecnico di Torino, Torino, Italy
[26] Dipartimento di Scienze Matematiche e Informatiche, Scienze Fisiche e Scienze della Terra, Università di Messina, Messina, Italy
[27] INFN-CNAF, Bologna, Italy
[28] INFN Trento Institute for Fundamental Physics and Applications, Trento, Italy
[29] Dipartimento di Matematica e Fisica, Università del Salento, Lecce, Italy
[30] Dipartimento di Scienze Fisiche, della Terra e dell'Ambiente, Università di Siena, Siena, Italy
[31] CNR, Istituto di Fisica Applicata "Nello Carrara", Sesto Fiorentino, Italy
[32] Dipartimento di Fisica, Università della Calabria, Rende, CS, Italy
[33] Dipartimento di Fisica, Università di Genova, Genova, Italy
[34] INFN, Laboratori Nazionali del Gran Sasso, Assergi, Italy

Received: 1 April 2020 / Accepted: 7 July 2020
© The Author(s) 2020

Published online: 24 July 2020

Abstract The goal of the PolarquEEEst experiment was to measure the cosmic charged particle rate at latitudes greater than 66° N, where no systematic and accurate measurements at sea level have ever been performed. A latitude range well above the Arctic Circle was explored on board of a sailboat, up to the unprecedented northernmost value of 82°07′ N. In this paper a description of the experimental set-up is reported, then the procedures for calibration and data analysis are described in detail. The results show that the rate measured in this latitude range stays constant within a novel accuracy of ±1%.

1 Introduction

The PolarquEEEst experiment measured with unprecedented precision the cosmic charged particle rate at sea level in a latitude range between 66° N and 82° N, well beyond the Arctic Circle. The interest of the measurement lies in the fact that it is well known to exist a significant dependence of the cosmic ray intensity at the ground level on latitude. In fact, the shielding effect due to the presence of the geomagnetic field, related to its roughly dipolar nature, is responsible of the fact that approaching the Equator, cosmic charged particles need higher and higher energy to reach the Earth surface, and consequently only a fraction of them reaches the ground. This induces a decrease of the flux of cosmic rays with decreasing latitudes. Vice versa, close to the Poles, the measured cosmic ray flux at sea level should reach its maximum level. However, above a latitude of around 50°, a saturation is observed, due to the combined effects of the geomagnetic cut-off in these regions, and of the shape of the cosmic particle energy spectrum [1].

In 1933, A.H. Compton compiled a detailed list of the available measurements of cosmic rays rates, mainly obtained by means of ionization chambers, versus both altitude and latitude [2]. The data came from multiple campaigns of measurements performed by various groups, nevertheless they clearly showed an increase of the measured cosmic rate at the ground level with latitude and, even if the statistic available at latitudes $> 60°$ N was very limited, a tendency to flatten above latitudes corresponding to the Arctic Circle. Moreover, in Compton's paper, data were compared to the Lemaître-Vallarta model [3], that, indeed, also predicted a flattening above around 50° (North and South).

The flattening of the intensity was also measured, more recently, by other experiments, mostly using neutron detectors, located on ground or on board of scientific or commercial ships, typically up to maximum latitudes of about 60° (for an interesting review, see, again, [1]). Nevertheless, even nowadays, scarce measurements are available above the Arctic Circle, particularly concerning charged particles, and more data, possibly on a longer time scale, are needed.

The PolarquEEEst experiment was hosted on the 60-feet eco-friendly sailboat Nanuq, which left for a six weeks cruise on July 22, 2018, from Ísafjörður (Iceland), reached Longyearbyen (Svalbard Archipelago, Norway), then circumnavigated the Svalbard Archipelago reaching the maximum latitude of 82°07′ N, and ended its voyage on September 4, in Tromsø (Norway). In addition to the detector on board the sailboat Nanuq, PolarquEEEst consisted in two other identical detectors, located in Norway and in Italy and used for cross-reference.

The sailing cruise was organized as the Polarquest2018 expedition [4]. The mission of Polarquest2018 was to celebrate the 90^{th} anniversary of the unfortunate Airship "Italia" expedition, which in 1928 performed an exceptional endeavor reaching by air the North Pole, but wrecked during its way back due to adverse meteorological conditions. The airship "Italia" expedition was not only an exploratory mission but also a scientific one, and the scientists on board carried out several scientific experiments, including measurements on cosmic rays flux performed quite close to the sea level, using an electroscope, without finding relevant changes within the explored latitudes [5].

Three scientific experiments were hosted on board the sailboat Nanuq: one related to the search for macro and microplastics in the Arctic sea waters around Svalbard (carried out by the CNR-ISMAR), another for cartographic mapping with drones of the north coast of the archipelago (by GREAL - European University of Rome and Italian Geographical Society, see [6]), and the third, conventionally called PolarquEEEst, about cosmic rays, whose description and first results are reported in this paper. A tale story of the mission and some photos are available in Ref. [7].

The PolarquEEEst experiment was carried out within the "Extreme Energy Events: Science inside Schools" (EEE in the following) project of the "'Museo Storico della Fisica e Centro Studi e Ricerche Enrico Fermi" (Centro Fermi, for shortness) in Rome [8], which also operates a large network of cosmic ray telescopes located across Italy and CERN.

In this paper the PolarquEEEst detector hardware, readout system and data acquisition will be thoroughly described. Data analysis procedures and relative physics results will then be presented.

2 The EEE project and the PolarquEEEst detectors

The EEE project started in 2004 as the first experiment on cosmic rays which, at the same time, includes an important

[a] e-mail: marcello.abbrescia@ba.infn.it (corresponding author)
[b] e-mail: Marionicola.Mazziotta@ba.infn.it (corresponding author)
[c] e-mail: Francesco.Noferini@bo.infn.it (corresponding author)

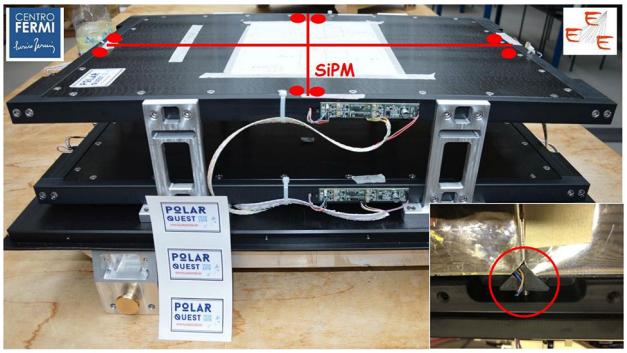


Fig. 1 One of the three PolarquEEEst detectors. The lines indicate the 4 tiles inside the internal light-tight box; the red points the position of the SiPMs. The small insert shows the cut on the scintillators (wrapped with mylar) and the wedge carved into the scintillators to ensure a good contact to the SiPM (red circle)

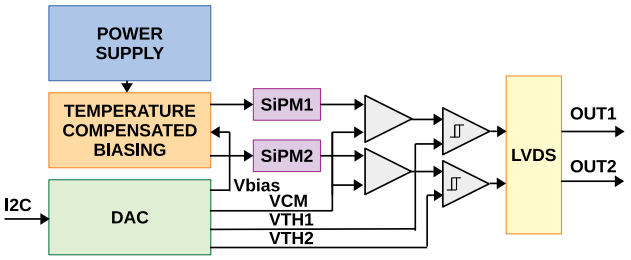


Fig. 2 Simplified block diagram of the FE card, showing its main components

component of scientific dissemination within high schools [9].

The EEE detectors are Multigap Resistive Plate Chambers (MRPC), derived from the time of flight detectors of the ALICE experiment at CERN. Three stacked chambers constitute an EEE "telescope", capable of tracking cosmic muons, and equipped with control, trigger, readout, and GPS modules. Presently 51 telescopes are operating in high schools all across Italy, while eight additional telescopes are installed in research laboratories, including two at CERN. The geographical area spanned by these telescopes exceeds 3×10^5 km^2, namely the largest area in the world used for such kind of experiments. In order to operate as a real network, all collected data are sent in real time to the INFN CNAF computing center for storage and reconstruction [10].

The EEE experiment is currently carrying out a large variety of measurements on cosmic rays. In particular, the topology of the array offers both the possibility to study the local cosmic rays flux, measured by means of single telescopes (see, for instance [11,12]), and to detect high or very high energy atmospheric showers (known as Extensive Air Showers), by searching events coincident in time across telescopes located few hundred meters up to few kilometers apart [13]. Moreover, due to the large surface spanned, EEE is in an almost unique condition to search for large distance correlations between showers, namely events detected almost at the same time in telescopes hundreds of kilometers apart, which would be potentially very interesting due to their peculiar origin [14].

The outreach part of the EEE experiment involves the students in the MRPCs construction and tests at CERN, in their installation at the schools, and in the responsibility to monitor the stations on a daily basis. The activities of the students also include masterclasses on data analysis, project conferences both via video-connection (monthly) and by presence (yearly). All students can access the collected data via a specifically developed web interface. Every year more than a thousand students and teachers participate in the project.

The PolarquEEEst experiment was conceived with the same philosophy of EEE, as a high level scientific program but also as an outreach initiative for high school students.

2.1 The PolarquEEEst detectors

The detectors for PolarquEEEst were developed respecting the constraints in terms of dimensions, weight, power consumption, and the requirements on robustness and reliability deriving from the fact that one of them had to be hosted on board of a sixty-feet sailing boat, cruising for six weeks with limited support and possibility to replace components. In particular, due to the eco-friendly nature of the mission, the total electric power available on the boat was limited, and the one assigned to the PolarquEEEst detector on board less than 20 W. Nevertheless the detectors had to be characterized by high efficiency and by the possibility to precisely tag the events in time and space in order to produce a detailed map of the cosmic ray intensity during the trip.

The choice fell on detectors made each of two layers of plastic scintillator (1 cm thick BC400 Saint-Gobain) separated by 11 cm, each divided into four tiles 20×30 cm^2 in dimensions. Each tile is readout by two AdvanSid ASD-NUV4S-P-40 Silicon PhotoMultipliers (SiPMs for shortness) placed on opposite corners of the tiles (whose angles were slightly cut), with a specifically designed mechanical wedge to firmly press the SiPM onto the scintillator surface, as shown in Fig. 1. Given the geometrical configuration chosen, these devices can detect charged particles coming from direction forming a maximum angle up to $\approx 73^\circ$ with the vertical. Of course, the detector acceptance is maximum for particles coming from the vertical direction and progressively decreases with the zenithal angle.

The four tiles were placed inside a light-tight box made of DELRIN®; the two layers were mounted on supports and the whole detector placed inside another external light-tight box of dimensions $560\times780\times195$ mm^3. One detector total weight is about 65 kg.

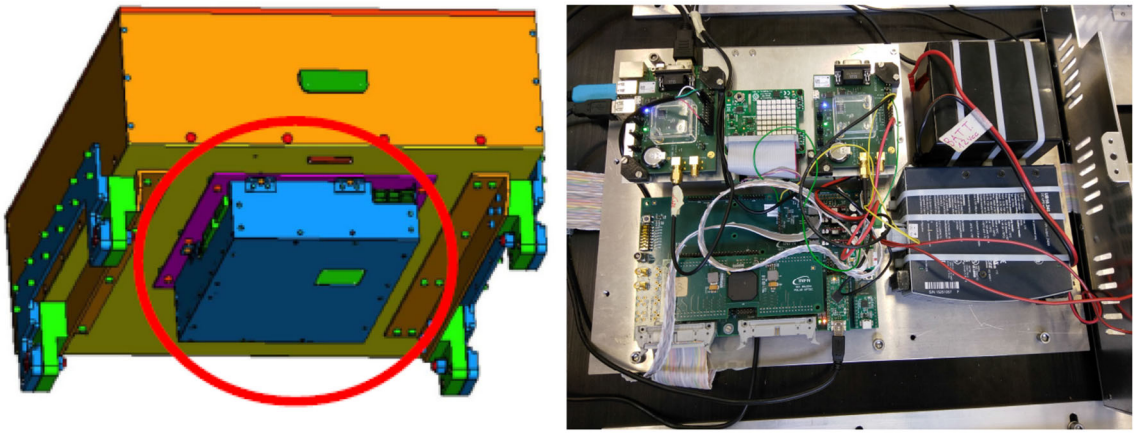


Fig. 3 Left panel: artist view of the detector box, with the electronics box at the bottom (highlighted with a red circle). Right panel: electronics box with the TRB, the power supply, the RPi3, the Sense Hat and the EVK-M8xZOE GLONASS board

The SiPMs are readout by Front End electronics (FE) custom cards, each able to independently process the analog signals from two SiPMs. Each card is equipped with two input pre-amplifiers, re-scaling the analog signals and feeding them to the discriminators. The thresholds of both discriminators can be remotely adjusted via a Digital to Analog Converter (DAC). The final stage of each FE card (eight in total for one whole detector) provides two independent low-voltage differential signals (LVDSs) to a custom Trigger and Readout Board (TRB), described in details in the following. The FE card hosts also a DC-DC stage, providing the necessary bias voltage to the two SiPMs. The bias is adjustable in the typical working range for the AdvanSid ASD-NUV4S-P-40, allowing a fine tuning of the gain for all the SiPM reading out the detector.

The FE card is also equipped with a stage for the temperature-related corrections to the SiPM bias. In fact, the dependence of the gain on temperature variations is a well known feature of SiPMs. The ASD-NUV4S-P-40 shows a linear dependence between the breakdown voltage and the temperature, with a typical gradient of 26 mV/°C between −20 °C and +50°C. The correction stage probes the temperature by means of a thermo-resistor and applies an adjustable linear correction to the SIPMs bias voltage. While thresholds and biases can be remotely tuned via the DAC, the temperature correction has to be set through a potentiometer installed onto the board, in order to avoid any accidental variation of the correction during the data taking. A simplified block diagram of the FE is shown in Fig. 2.

The three PolarquEEEst detectors were conventionally called POLA-01, the one on board the sailboat Nanuq, and POLA-02 and POLA-03 the ones located on ground.

2.2 The low power consumption Trigger and Readout Board

The readout electronics, the power system and the data acquisition system (DAQ) for the PolarquEEEst detectors are hosted in a box located at the bottom of the devices (see Fig. 3). In order to comply with the above requirement about the limited power supply available on board, the system was designed so that its total power consumption is about 12.5 W.

The 16 SiPM LVDS signals from each detector are fed into the Trigger and Readout Board (TRB), which is equipped with an Altera Cyclone 5 Field Programmable Gate Array (FPGA) [15], a high performance Multi-Hit Time-to-Digital Converter (HPTDC) [16], and an USB card with a FT232H chip [17] (see Figs. 4 and 5).

The TRB board is powered with 12 V voltage, and feeds the main 5 V power to all the electronics through a DC-DC converter hosted on board. For POLA-01, on the boat, the 12 V was obtained from the available 24 V by means of a second DC-DC converter. For the two other detectors on the ground, POLA-02 and POLA-03, in order to keep a similar power configuration, an AC-DC was used to convert the 220 V to 24 V. In addition, a backup battery was used in case of temporary power down.

The event trigger is implemented within the FPGA, by requiring at least three SiPM signals to be in a 10 ns time-coincidence window. Moreover, the trigger logic requires two of the SiPMs to be from the same tile and another from a tile in the other plane. In case of need, noisy SiPM can be excluded by the trigger logic. For testing purposes, the trigger can also be generated by an external pulse or via software.

In the FPGA, an algorithm to calculate the arrival time of each SiPM LVDS signal and its start-to-end time duration is also implemented. This directly provides a Time-Over-Threshold (TOT) measurement, namely the interval between

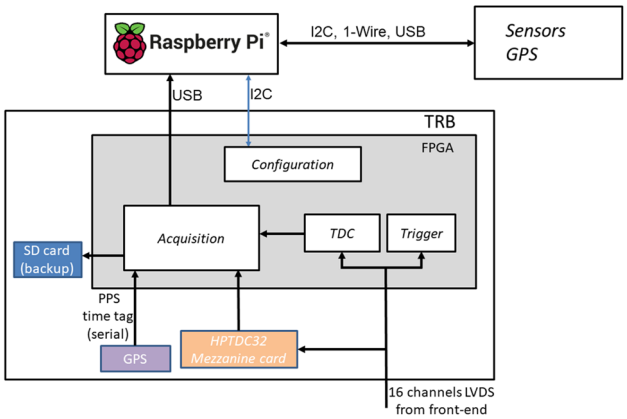


Fig. 4 Read-out DAQ and Control block diagram

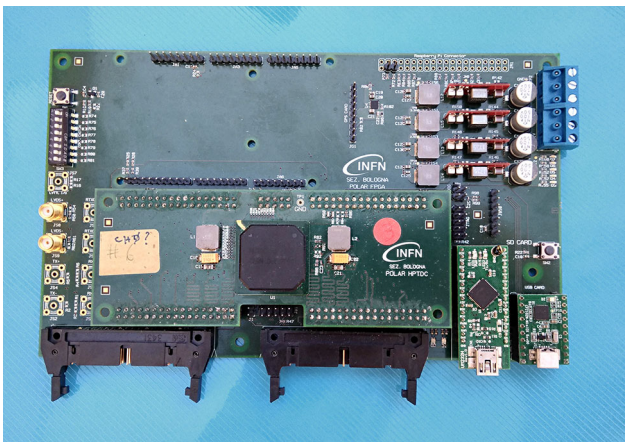


Fig. 5 Photo of the Trigger and Readout Board (TRB)

the time when a signal from the SiPM exceeds the threshold, and the time it crosses it down again, which is approximately proportional to the charge of the signal. The same measurement is performed with the HPTDC. FPGA and HPTDC provide a redundant measurement, quite important in such type of experiments.

All coincidences capable of generating a valid trigger, and all acquired event triggers, are counted by two separate counters implemented in the FPGA. By comparing the counts from the two scalers, the dead time can be calculated.

2.3 Sensors and DAQ

Either a GPS (Global Positioning System) or a GLONASS (GLObal NAvigation Satellite System) board is used to provide the position, the absolute time and to provide a 1 pulse-per-second (PPS) to the TRB. A 100 MHz system clock is also used by the TRB to provide a precise event timestamp, together with the PPS. An EVK-M8xZOE GLONASS board [18] was used for POLA-01, while for POLA-02 and POLA-03 a GPS board with L80-M39 module [19] was employed.

The DAQ is controlled by a Raspberry Pi 3 B+ board (RPi3) [20], which controls the TRB through a I^2C connection and receives data via USB from the FT232H card.

Several sensor modules, connected to the RPi3, are used to monitor the temperature, the pressure and the orientation. In particular, three DS18B20 1-Wire digital thermometer sensors are used to monitor the temperature inside the electronics box, inside the detector box, and outside. Both the bare chip [21] and the waterproofed versions [22] of the DS18B20 sensor were used.

A Sense Hat board, made especially for the Astro Pi mission [23], is used to monitor the orientation (yaw, pitch, roll) via an accelerometer, a 3D gyroscope, and a magnetometer with the LSM9DS1 sensor [24], the pressure with the LPS25H sensor [25], and the humidity with the HTS221 sensor [26].

For redundancy, a BME280 sensor [27,28] is also used to monitor the pressure, the temperature and the humidity, and a BNO055 sensor [29] is also used on POLA-01 to monitor the orientation of the detector.

Python scripts running on the RPi3 are used to readout the TRB and the sensors, and to store the data on the RPi3 SD card. Several python scripts are also used to configure the TRB and the FE DAC, and monitor in real time the data with the RPi3. Also a web-interface for the data acquisition is used.

3 PolarquEEEst detector commissioning and installation

The three PolarquEEEst detectors were built at CERN in May 2018. The mechanics, scintillators, SiPM and Front-End parts were assembled with the involvement of 23 high-school students from Italy, Norway and Switzerland, as similarly done for all EEE detectors.

After assembling, POLA-01, POLA-02 and POLA-03 were tested for a month long period, first in stand-alone and then also using the two EEE telescopes located at CERN, named CERN-01 and CERN-02, as benchmarks. The three POLA detectors were placed side by side, at a position a few tens of meters from the two EEE CERN telescopes.

Usual basic checks were performed by verifying, for instance, that the measured frequencies of the impinging particles were roughly consistent among the three detectors. At this stage, also, the thresholds and bias voltages of all SiPM channels were precisely set by slightly tuning them with respect to their default values, in order to get the Time-Over-Threshold (TOT) and Pseudo-Efficiency (PE) distributions similar for all channels in the three detectors.

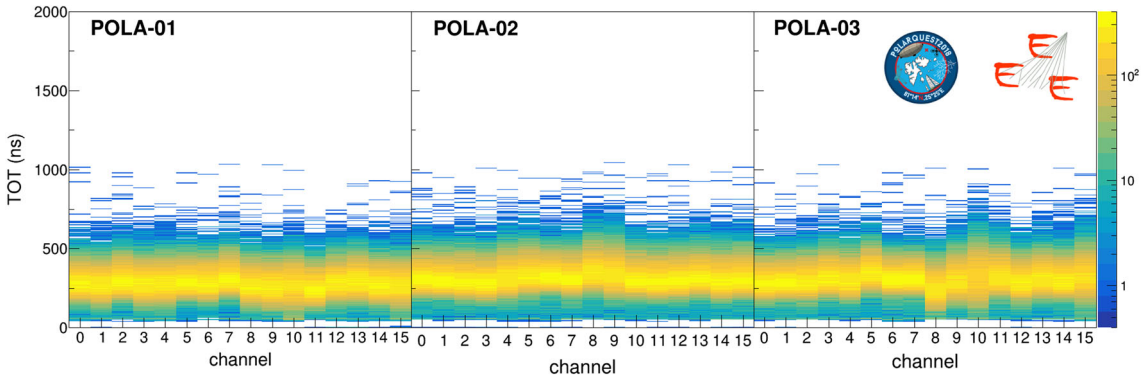


Fig. 6 TOT distributions for POLA-01, POLA-02 and POLA-03. All plots refer to data taken on July 27, 2018. The channel numbering scheme is explained in the footnote

Examples of TOT distributions after equalization are shown in Fig. 6; they are quite similar across the various channels of the three POLA detectors [1].

The PE of a channel is defined as the probability that a SiPM provides a signal, on the condition that the other SiPM, reading the same scintillator tile, contributed to the same event trigger. Such a quantity can be easily measured during data taking since, as already pointed out, the trigger was based on the request that at least three SiPMs over four candidates of two tiles on two planes (*majority* condition) provided a signal in coincidence. Since two SiPMs coupled to the the same tile see the same events, events with a larger number of photons are likely to be detected by both SiPMs. There are also positions where an impinging crossing particle is detected more efficiently by the closest SiPM and less by the farthest. These effects are small (of the order of a few per cent of the cases), but imply that, although PE is not an absolute measurement of the channel efficiency, nevertheless it can be quite useful to detect macroscopic problems during operations and to monitor channel stability.

An example of PE value as a function of the channel number is shown in Fig. 7; it always stays close to 1. Also the fraction of events out of time are reported in Fig. 7, meaning the fraction of events where a signal from a certain SiPM channel was detected, but fell out of the 10 ns time window where coincidences for triggers were searched for. Looking for them in a time window of ± 100 ns around the trigger, as was done in this case, they were generally less than 1 %. This immediately gave an estimate of the noise in the channels and the amount of accidentals, which resulted to be negligible.

TOT and PE equalization was also repeated once the detectors were installed at their final destinations, and used later on for monitoring purposes (see next Section).

During the period when the detectors stayed at CERN, the GPS time tags, in particular, were carefully checked, in order to be sure that the time reconstruction chain worked properly.

A plot of the events detected in coincidence by POLA-01 and CERN-01 is reported in Fig. 8. The plot refers to events acquired on June 17, 2018, for a period of about 11 h, and was obtained by using the time tags associated to each event in the two detectors and checking if there was any pair with a difference in time less than ± 1 μs. In the figure the peak due to the particles associated to the same Extensive Air Shower impinging on both detectors can be clearly seen above the background due to accidentals.

The observed width of the peak, around 74 ns, is due to two main contributions: the intrinsic time precision of the two detectors, and the time spread due to the uncertainty on the arrival direction of the shower front. The intrinsic time precision refers to the accuracy of the absolute Universal Time Coordinate (UTC) each event is tagged with, and is given by the detector time resolution convoluted with the GPS timing precision. The UTC tag is used to perform offline coincidences among the detectors.

Since the two detectors were around 70 m apart, the spread due to uncertainty on the shower arrival direction can be estimated to be about $\pm$ 50 ns, and that allows to infer an intrinsic time precision of the two systems around 50 ns.

Analogous plots, also obtained with data taken on June 17, 2018, and referring to the coincidence peaks between two pairs of POLA detectors, namely POLA-01/POLA-02 and POLA-01/POLA-03, are shown in Fig. 9. In this case, since the POLA detectors were placed less than a couple of meters from each other, the intrinsic time precision only determines the width of the coincidence peak, resulting in a value between 40 and 50 ns, also coherent with the previous observations. Both plots correspond to a simultaneous data

[1] The channel numbering scheme, used here and in the following Figures, groups together SiPMs from the same side of the two scintillator planes. So, 0 and 1 channels label the two SiPMs of one of the long side of the top scintillator plane, and 2 and 3 the corresponding SiPMs on the bottom plane. 4 and 5 label the SiPMs on the short side of the top plane, moving counterclockwise, 6 and 7 the corresponding on the bottom plane, and so on, covering all the sixteen channels for each detector.

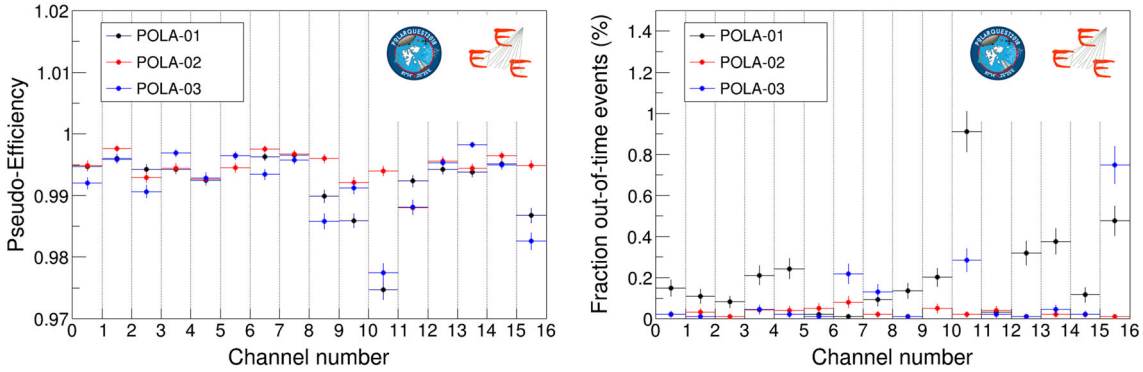


Fig. 7 Left: Pseudo-Efficiency, channel-by-channel, for POLA-01, POLA-02 and POLA-03. Right: Fraction of events out of time, channel by channel, for the three POLA detectors. All plots refer to data taken on July 27, 2018

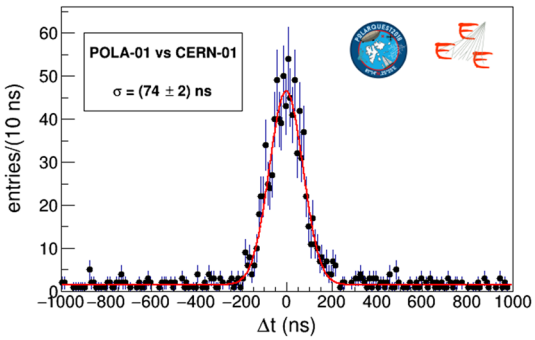


Fig. 8 Time coincidences between POLA-01 and CERN-01; data were taken on the June 17, 2018

taking period of about 2.5 h, the difference between the number of coincidences observed in the two cases being mainly due to the fact that POLA-01 was closer to POLA-02 than to POLA-03.

After the period at CERN, POLA-01 was shipped to Isafjörður in Iceland, and mounted on the deck of the Nanuq sailboat, inside a hutch specifically designed to host it, positioned just above the sleeping berth and open toward it: being connected to the cabin and directly accessible from it, the detector and its electronics were protected against external weather conditions and measured a temperature excursion less than 10°C. The upper layer of the hutch was mainly made of birch plywood (12 mm), fibre glass (1.8 mm), polystyrene foam (80 mm) (see Fig. 10). These are to be added to the 2 cm of plastic used for the black box enclosing the scintillators to estimate the total amount of material above them.

At the same time, POLA-02 and POLA-03 were installed inside two high schools, one at Nesodden, close to Oslo in Norway, at 59°50′ N, 10°68′ E, 84 m of altitude and the other at Bra, in Piedmont (Italy), at 44°42′ N, 7°52′ E, 310 m of altitude, respectively, where they were constantly monitored and controlled by teams of local teachers and students. POLA-02 and POLA-03 were hosted in air-conditioned rooms, where temperature was kept constant with a precision of around 1°C, and permanently connected to the internet, so that data could be transferred in real time, and the devices could be accessed remotely. Moreover, rooms on high floors of the schools buildings were chosen, in order to minimize the muon absorption in the overlying rooftops. At Nessoden the ceiling above POLA-02 was mainly made of plaster panels (12.5 mm thick), glass wool, and a metal layer on top of which a 22 mm particle board and two layers of cardboard were placed. At Bra, the material above the POLA-03 detector was a 20 cm layer of full bricks, 5 cm of plasterboard and an additional layer of terracotta tiles.

4 Data taking and detector monitoring

The official data taking period of the PolarquEEEst mission has been defined to start at 00:00:00 of July 21, 2018, namely the day before when the Nanuq set sail from Isafjörður with POLA-01 on board, at geographic coordinates of 66°04′ N, 23°07′ W, and to last until 23:59:00 of September 4, 2018, at end of the day when it arrived at Tromsø, at 69°39′ N, 18°57′ E. Plots of the relevant quantities vs. time shown in this paper will be mainly referred to this period of time. Of course, the three POLA detectors took data, whenever possible, also before July 21. After its arrival at Tromsø, POLA-01 was switched off and dismounted from Nanuq, while POLA-02 and POLA-03 remained at their locations taking additional data.

Given the sensitive materials used for these detectors, only charged cosmic particles were detected, namely basically muons and a reduced fraction of electrons. Particles detected by the PolarquEEEst detectors are residuals from Extensive Air Showers generated by primary cosmic particles entering and interacting in the atmosphere, which produce, in a cascade process, multiple secondary particles of which only a fraction actually arrive to impinge onto the ground.

The fractions of muons and electrons, and their energy, were affected by the material above the detectors, which was

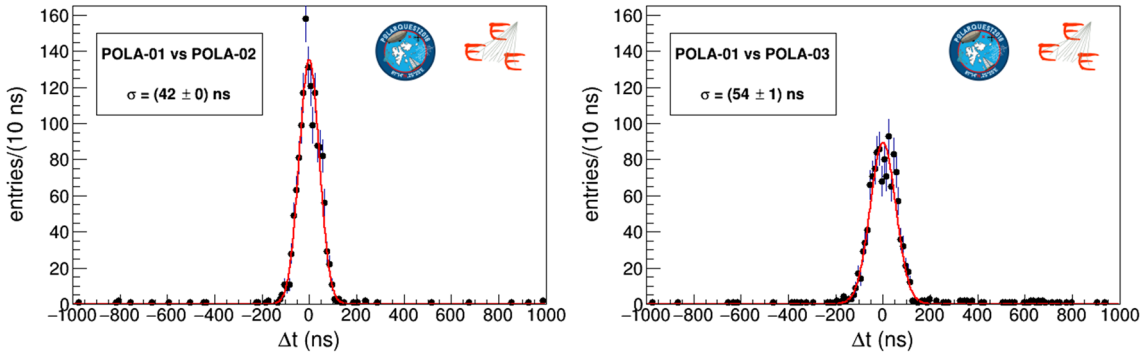


Fig. 9 Time coincidence peaks of POLA-01/POLA-02 (left) and POLA-01/POLA-03 (right). Data were taken on June 17, 2018 and correspond to approximately 2.5 h



Fig. 10 Photo of the POLA-01 detector enclosed in its fiberglass yellow hutch on the deck of the Nanuq sailboat. (*Photo by O. Pinazza.*)

not the same in the three cases. Anyhow, it was not possible to disentangle the contribution from the two species. Moreover, the detectors were characterized by a very limited tracking capability, provided only by the information about which tile of the upper and lower scintillator planes yielded a signal, information which, anyhow, was not exploited in this analysis.

Data taking was performed in short runs, of 30000 "buffers" each, that were saved on the solid state memory of the devices immediately after the conclusion of each run, in order to reduce the possibility of losing data because of hardware failures. A "buffer" is a set of data read out from the TRB all together at the same time, which can contain either one or more triggered events. On the average, 30000 buffers corresponded to about 38500 triggered events. On August 14, the number of buffers in one run of POLA-01 was increased to 50000, to reduce the total number of files to be handled.

For the analysis described in this paper, only runs containing more than 9000 buffers and characterized by a dead time less than 0.25% were considered. This allowed to exclude short calibration runs or runs affected by some kind of hardware or software problem.

The two detectors installed at high schools, POLA-02 and POLA-03, were configured to transmit data to the EEE computing center at CNAF (Bologna). According to the usual EEE workflow, data were processed and reconstructed and several quality plots were soon thereafter published on the web monitor page [30] to verify that the data acquisition system was working properly. This allowed a continuous monitoring of these devices.

When POLA-01 was hosted on Nanuq sailing in the Arctic Sea without any stable internet connection, the data acquired were stored in the local solid state memory and later on transferred as soon as an internet connection was available (this usually happened when the boat was harboured in a port). In order to replicate also for POLA-01 the frequent data quality checks, data were daily reconstructed and checked locally by the researcher on board using a laptop connected to one of the USB port of the Raspberry PI. Moreover, the Data Quality Monitor plots (few tens of kBytes in size) were sent to CNAF using a satellite phone whenever possible.

During the 46 days of official data taking, corresponding to 1104 h, the POLA-01 detector acquired about 110 millions of events, POLA-02 131 millions, and POLA-03 109 millions.

The continuous monitor of the activity of the three PolarquEEEst detectors during the full period allowed to keep the duty cycle of POLA-01 at the level of 89.1%, (equivalent to 984.7 h of effective data taking) and the duty cycles of the two other telescopes almost at 100%, and precisely 99.5% for POLA-02 (equivalent to 1098.1 h of data taking) and 98.6% for POLA-03 (1088.2 h).

Main reasons for downtime in POLA-01 were occasional power cuts, bad weather, or various GPS, sensors, TRB and DAQ problems which typically needed just a reboot of the system to be solved. Moreover, during bad weather it was sometimes impossible to connect the laptop on board to POLA-01, and this happened to cause some data loss because the DAQ stopped and needed to be restarted. The cuts on run quality cited above contribute to the total dead time for about 0.25%.

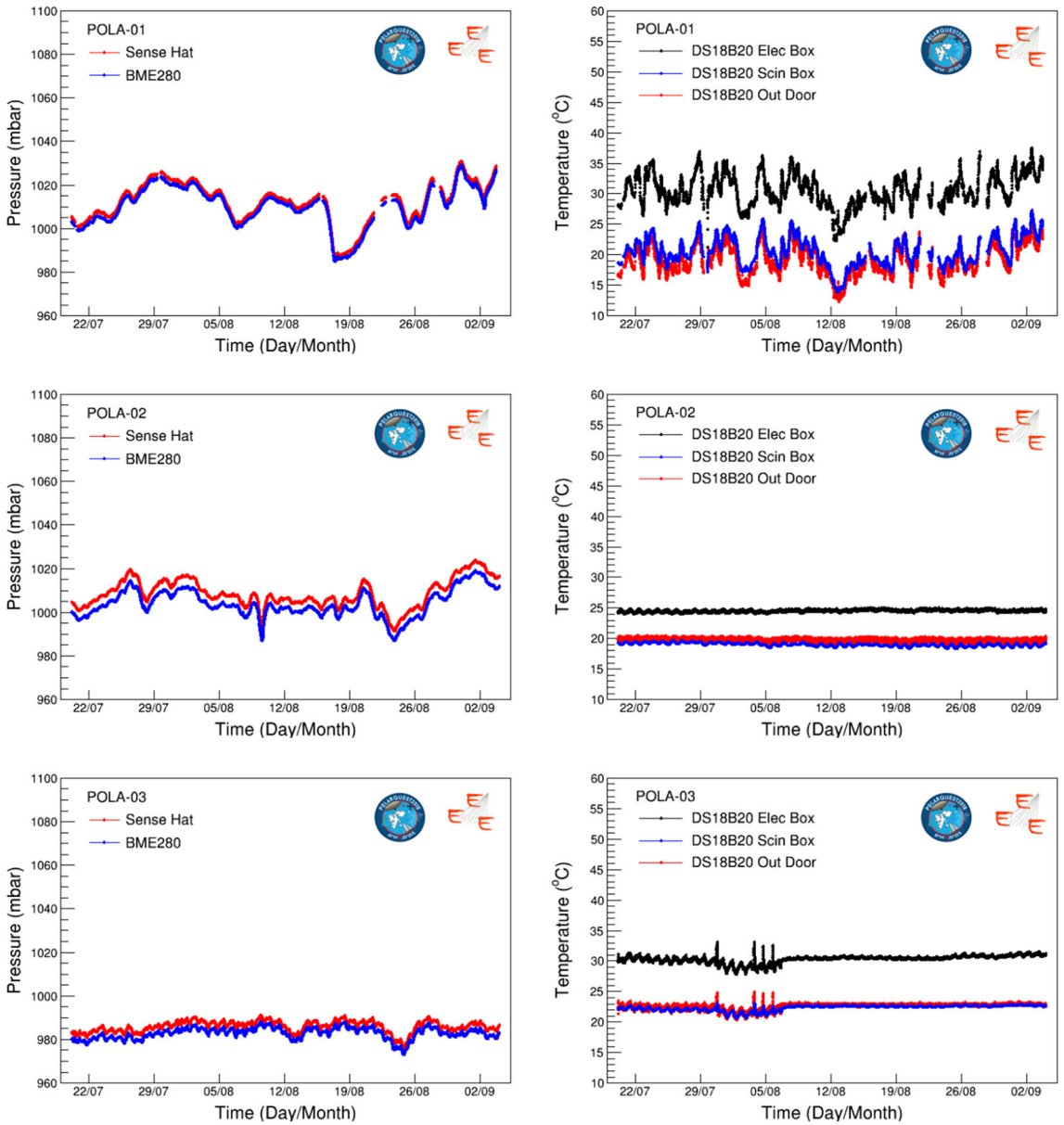


Fig. 11 Pressure (left) and temperature (right) as a function of the time, from July 21, 2018 up to September 4, 2018, measured by the sensors of the three POLA detectors: from top to bottom, results from the sensors of POLA-01, POLA-02 and POLA-03

Environmental parameters were continuously measured during operation, since these are important for possible correlations with the measured flux of cosmic muons and, in general, to have a clear picture of the conditions these devices were operating at.

Sensors of temperature, pressure, etc. were readout during data taking at fixed time intervals, namely every 2 s for POLA-01, and every 30 s for POLA-02 and POLA-03. In fact, environmental conditions were expected to vary more rapidly for POLA-01 with respect to the others and, in particular, frequently measuring the inclination of the detector with respect to the vertical due to the boat roll and pitch was critical, as it will be shown later on in this paper.

Pressure and temperature measured by the sensors of the three detectors POLA-01, POLA-02 and POLA-03, since July 21 to September 4, 2018, are shown in Fig. 11 as a function of time. For the sake of clarity, quantities reported in the plots of Fig. 11 are sampled at time intervals of 10 min.

For what concerns pressure, data both from the SenseHat and the BME280 sensors are plotted, and they basically coincide, apart from a few mbar systematic shift, more evident for POLA-02. Pressure for POLA-01 registered important excursion during the data taking, up to 45 mbar, while pres-

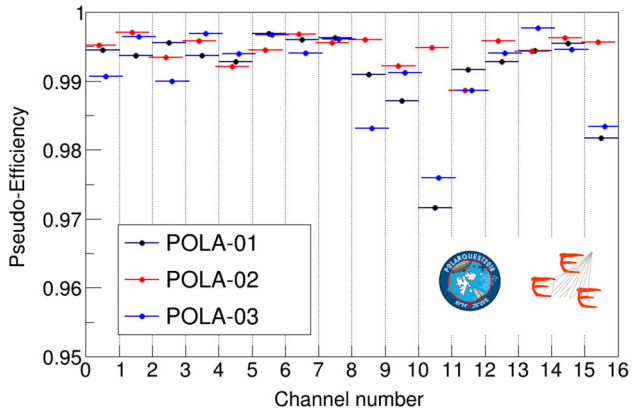


Fig. 12 Channel by channel PE averaged in the full period, for POLA-01, POLA-02 and POLA-03. Here, the binomial errors are used, to small to be visible

sure measured by POLA-03 was on the average 30 mbar lower than the others because Bra, where the detector was located, is 285 m a.s.l.

Temperature was measured, by means of three identical DS18B20 sensors, placed one inside the box hosting the electronics, another inside the box hosting the scintillators and the third outside it, glued on its outer surface, which basically measured the environmental temperature. While these two last temperature values are very close to each other, the one measured inside the electronics box is, as expected, significantly higher. These plots confirm the expected temperature excursions of $\pm 5°C$ for POLA-01 and $\pm 0.5°C$ for POLA-02 and POLA-03, apart from a few days period at the beginning of August 2018, when the air conditioning system of the room hosting POLA-03 was not operating correctly.

In addition to environmental conditions, also measured rates, TOT and PE were used to check the system stability. Examples of TOT and PE distributions were already reported in Figs. 6 and 7, while cosmic muon rates were the main goal of the measurements performed with these detectors, and will be extensively discussed in the following.

A summary of the measured PE, averaged over the full period of data taking, is given in Fig. 12, for the three detectors. PE remain higher than 97 % during the whole period of data taking in all channels, and, anyhow, short-term variations with respect to their average value stay well within a ± 0.5 % range.

Distributions obtained measuring the average TOT values (<TOT>), channel by channel, over 1 min time intervals, during the whole period of data taking, can be seen in the three plots of Fig. 13, and again, show a quite stable system behaviour. TOT distributions for POLA-01 are slightly lower than the others because the applied threshold were higher. Their spread is larger, probably due to the fact that POLA-01 operated in less controlled conditions with respect to POLA-02 and POLA-03, for instance in terms of material positioned around them, or the different cosmic particle spectrum when in open sea at different latitudes, or the fact that POLA-01, integral with the Nanuq sailboat, was not always horizontal.

Finally, the dependence of the PE on the <TOT> is shown in Fig. 14 for channel 0 of the POLA-01 detector, featuring variations smaller than 1%. The plot demonstrates that channel PE stays quite constant over a wide range of <TOT>. Similar behaviours are observed for the other channels of POLA-01 and all the other channels of the other detectors, implying that no macroscopic differences in efficiency are expected because of different <TOT> across the three POLA detectors.

Also the dead time due to the DAQ system was measured by comparing the number of triggers arriving in input to the TRB and the number of events actually written on the solid state memory, as already pointed out in Sect. 2.2. The fraction of events lost due to the dead time of the DAQ system is about 10^{-3}.

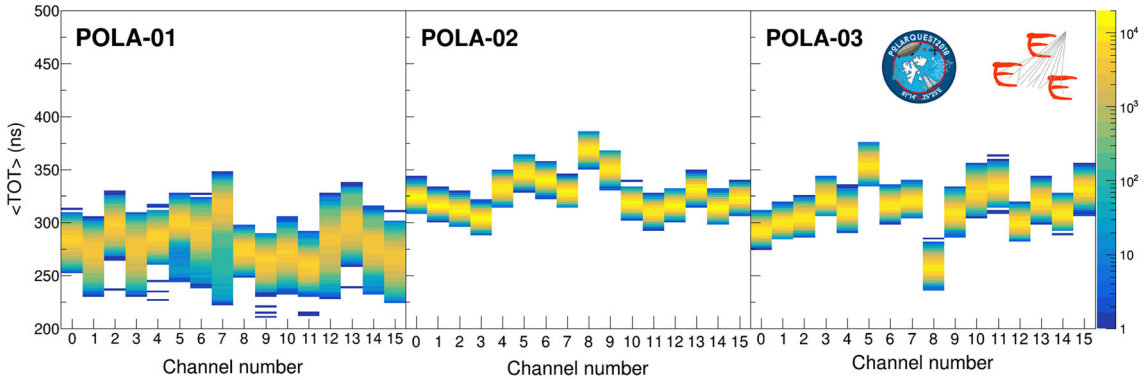


Fig. 13 TOT distributions averaged over the full period of data taking measured with POLA-01, POLA-02 and POLA-03

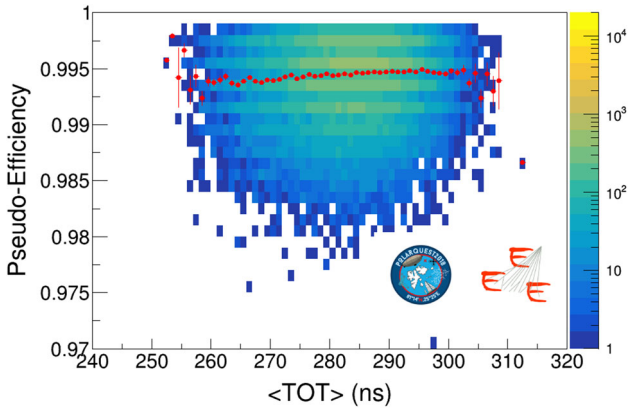


Fig. 14 PE vs. <TOT> for channel-0 of POLA-01. The red points represent the average PE values

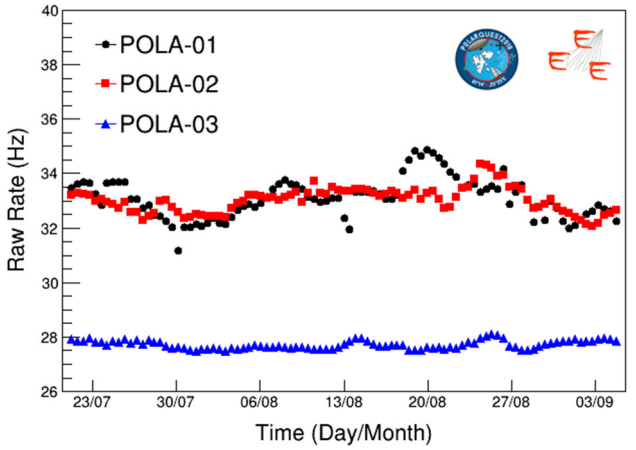


Fig. 15 Raw rate measured by POLA-01 (black circles), POLA-02 (blue squares) and POLA-03 (blue triangles) as a function of the time since July 22, 2018 till September 4, 2018

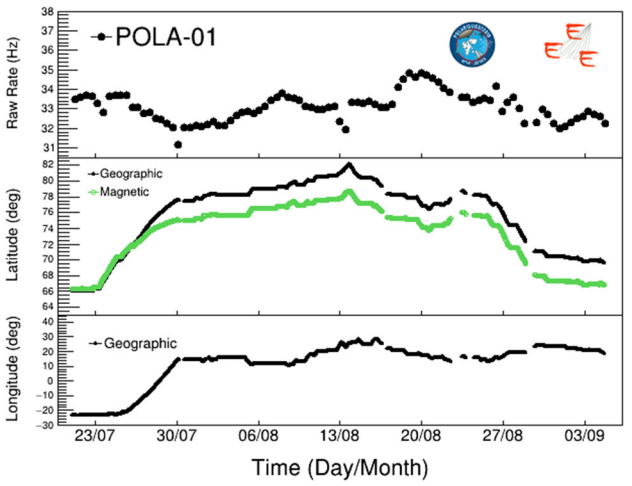


Fig. 16 POLA-01 raw rate (top panel), geographic and magnetic latitude (middle panel) and longitude (bottom panel) as a funtion of the time since July 22, 2018, till the end of its trip in Tromsø

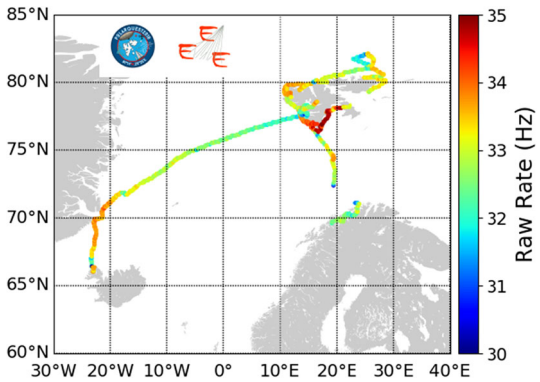


Fig. 17 Raw rate map measured by POLA-01 during its trip in the Arctic Sea

5 Corrections to the raw data

The rate of impinging particles as a function of the time (henceforth called "raw rate") measured by the three detectors of the PolarquEEEst experiment for the full period of official data taking is shown in Fig. 15. Raw rates were determined by counting the number of events contained in a certain run and dividing it by the run time duration. For the sake of clarity, to obtain each of the data points in Fig. 15 and in analogous plots thereafter, multiple runs have been grouped together in 12 h time slots, and the raw rate has been averaged over that time interval. As it can be seen from Fig. 15, POLA-01 and POLA-02 measured most of the time a raw rate between 32 and 34 Hz, sometimes with significant fluctuations outside this range, particularly for POLA-01, while POLA-03 stayed more stably around 28 Hz.

The raw rate measured by POLA-01 during its trip is also shown in Fig. 16, together with the detector geographic and magnetic latitudes, and geographic longitude, as a function of time. POLA-01 reached the maximum latitude, slightly above 82° N, in the evening of August 13, 2018. From this Figure there is no evidence of any correlation of the measured raw rate with geographical or magnetic coordinates.

A map showing the trip route of the Nanuq sailboat during its mission, with, in colours, the raw rate measured by POLA-01, is shown in Fig. 17. Apparently, a significant increase in the raw rate was measured when the boat sailed across the South coast of the Svalbard archipelago, and a slight decrease close to the maximum latitude reached, North of it.

Indeed, in order to compare data acquired by the three POLA detectors, positioned at various latitudes and altitudes, in different environmental conditions, it is important to correct the raw rates for all the local effects which can affect the measurements.

For instance, for POLA-03, the absorption of cosmic particles in the material above it is expected to be relevant, since the telescope was installed under a roof made of full bricks, while the others were located under thinner layers of lighter

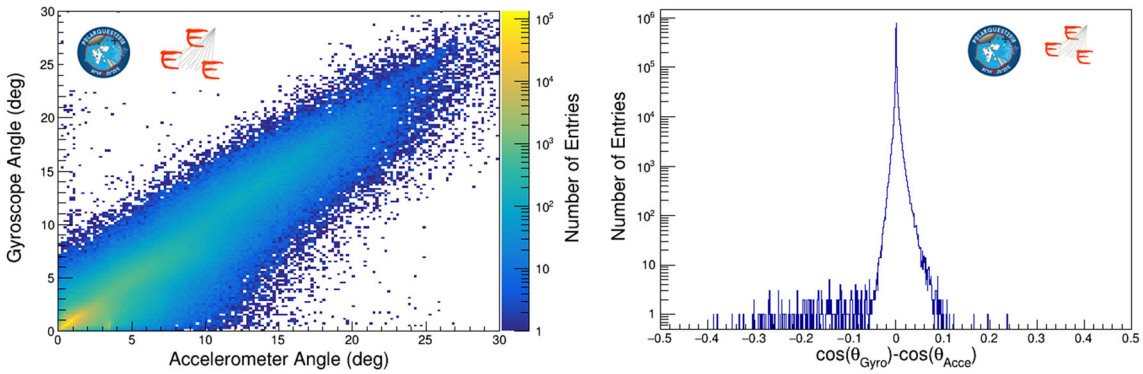


Fig. 18 Left: Correlation between the zenith angle measured with the gyroscope and by the accelerometer in POLA-01. Right: Distribution of the difference of the cosines of the two angles measured by the gyroscope and the accelerometer mounted on POLA-01

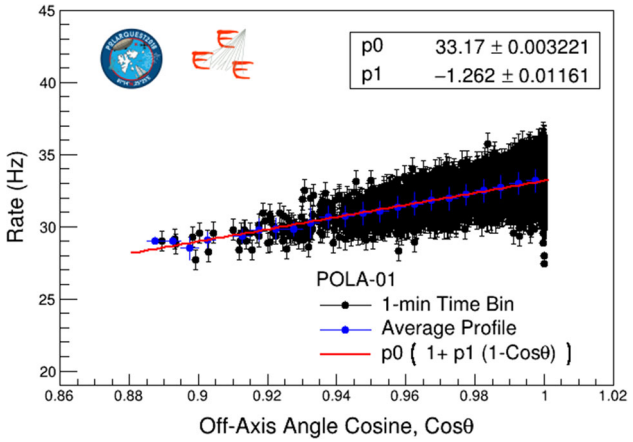


Fig. 19 POLA-01 rate as a function of the cosine of the angle between the vertical and the axis perpendicular to the top surface of the detector

materials. In order to estimate the absorption in the roof, some data were also acquired outside the building, for one day, before the official data taking started. The overall effect when moving POLA-03 from outside to its final position inside the building was measured to be at the level of ≈ 20%. This explains why in Fig. 15 the data points referring to POLA-03 are systematically lower with respect to the others.

A much smaller effect was expected for POLA-02, which had a much thinner roof on top of it. In fact, after performing a similar check, the rate variation of POLA-02 when moving it from outside the building to indoor was found to be at the level of ≈ 3%.

Temperature is well known to affect the gain of the SiPMs, and therefore its variation might affect the measured rates. However, since temperature excursions were limited in the experimental conditions of PolarquEEEst, even on the Nanuq, temperature effects during data acquisition were found to be low (surely less than 0.5%) and no significant variation of the rate with temperature was observed with the POLA detectors. This was also confirmed by laboratory tests with a climate chamber, performed with a spare scintillator tile after the expedition, where no relevant variation of the rate could be measured within the temperature excursions observed by POLA-01.

5.1 Correction for detector inclination

One important factor to be taken into consideration for POLA-01 is its inclination with respect to the vertical direction. In fact this device was mounted on a sailing boat which could pitch and roll depending on the weather and sea conditions, and the sailing pace chosen, and therefore could stay inclined during data taking for not negligible amounts on time. Detector inclination affects the measured raw rate because of its angular acceptance and the fact that the cosmic flux at sea level depends on the zenithal angle, namely a larger number of cosmic particles comes from directions close to the vertical.

Inclination was measured using both the gyroscope and the accelerometer, included in the Sense Hat hosted in the electronics box aside the Raspberry PI used for readout and shown in Fig. 2. A correlation plot of the angles θ_{Gyro} and θ_{Acce}, between the vertical direction and the axis perpendicular to the top surface of POLA-01, is shown in Fig. 18-left. For this plot all the measurements, taken each 2 s, were used. It shows that the cases where the two angles differ significantly, namely more than $1° \div 2°$, are of the order of few per million and might probably be due to sudden mechanical shocks during navigation that affected the gyroscope measurements for a few seconds. A distribution of the difference of the cosines of the two angles measured by the gyroscope and the accelerometer is also shown in Fig. 18-right, and confirms this conclusion.

The particle rate measured by the POLA-01 detector when it was not positioned horizontally depends both on the angular dependence of the cosmic rays flux on the zenith angle θ (which roughly follows a $\cos^2\theta$ law [31]), and the detec-

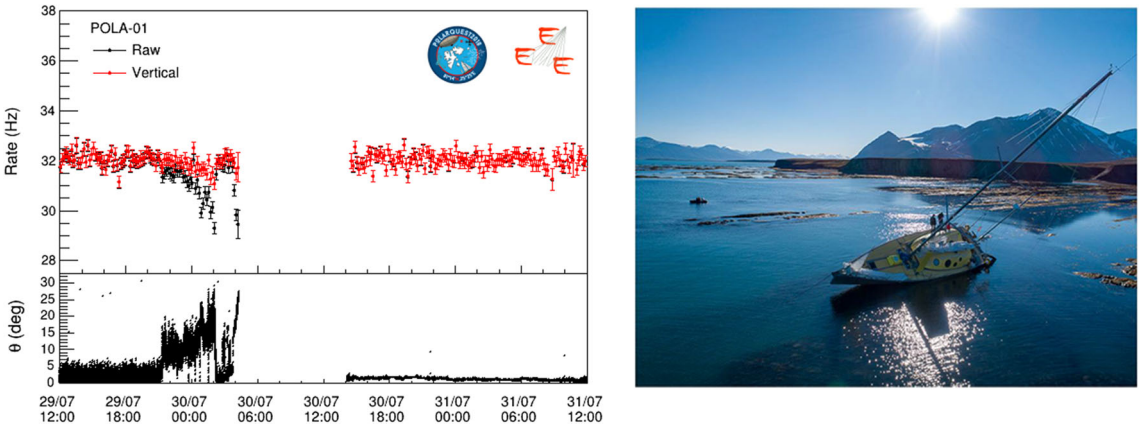


Fig. 20 Left: Raw rate measured by POLA-01 (black points in the upper plot) from July 29 to July 31, 2018, when the boat was inclined for a period of about 9 h. Also the rate corrected for the inclination effect (red points) and the inclination angle (black points in the lower plot) are shown. In this case, a 10 min binning has been used for the rate, while for the inclination angle measurements every 2 s are reported. The time is expressed in UTC. Right: A photo of the sailboat Nanuq during the incident of July 30, when the boat reached 48° inclination during low tide (*Photo by M. Struik*)

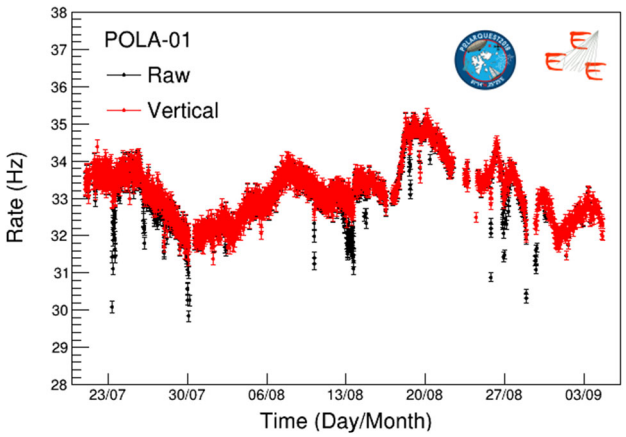


Fig. 21 POLA-01 rate as a function of time from July 22 to September 4, 2018. Black points: raw rate; red points: rate corrected for the inclination effect discussed in the text

tor geometrical acceptance around that zenith angle, which changes depending on the detector inclination. It has been verified that, in the angular range of interest here, the measured rate follows a simple $\cos\theta$ law, as shown in Fig. 19. For this figure, the whole data taking period has been divided in time slots of 1 min duration each, and the average rates and inclination angle in these time slots have been computed. Also a linear fit to average profile is superimposed in Fig. 19. Note that this is probably only a first order approximation of a more complicated law, valid in a wider range.

Therefore, in order to correct the raw rate, in this analysis, to each event in a run was associated a θ_{Gyro} value obtained by linear interpolation between the two measured θ_{Gyro} closest in time to the chosen event. Then, the number of events in a run was counted, weighting each event with the inverse of $\cos(\theta_{Gyro})$. The rate corrected for the inclination effect was obtained by dividing this number for the run duration.

In an alternative way, it has been also verified that, thanks to the large statistic involved, the results obtained do not change significantly if, simply, the raw rate of each run is divided by the average $\cos(\theta_{Gyro})$ measured during that run. Also using $\cos(\theta_{Acce})$ leads to the same results.

A striking opportunity to verify the importance of the correction for telescope inclination and of the accuracy of the procedure used, occurred when, on July 30, the Nanuq boat got stranded close to the Svalbard Islands because of low tide. The raw rate measured by POLA-01 during this event, and immediately before and thereafter, is shown in Fig. 20, together with the measured inclination angle. In the late evening of July 29 the boat started sailing upwind, more and more inclined, then changed pace, progressively returning to the vertical position. At 3:30 UTC of July 30 it got stranded, and a clear rapid reduction in the rate can be seen just in coincidence with this event. At around 30° of inclination, data acquisition had to be interrupted for safety reasons, even if the boat ended up to be inclined up to 48° bank with respect to the vertical, where it stayed for about 9 h, until the tide came back.

Anyhow, rate corrected for the orientation effect is also shown, and this stays approximately stable during the full period. The hole in the data acquisition that can be seen is due to the fact that all systems, including electrical power, were shut down for security reasons while waiting for the tide. Note that in this case, events have been grouped in 10 min bins, to compute the rates.

The raw rate measured during the whole period of data taking by POLA-01 and the rate corrected for the inclination effect are both shown in Fig. 21. The periods when such

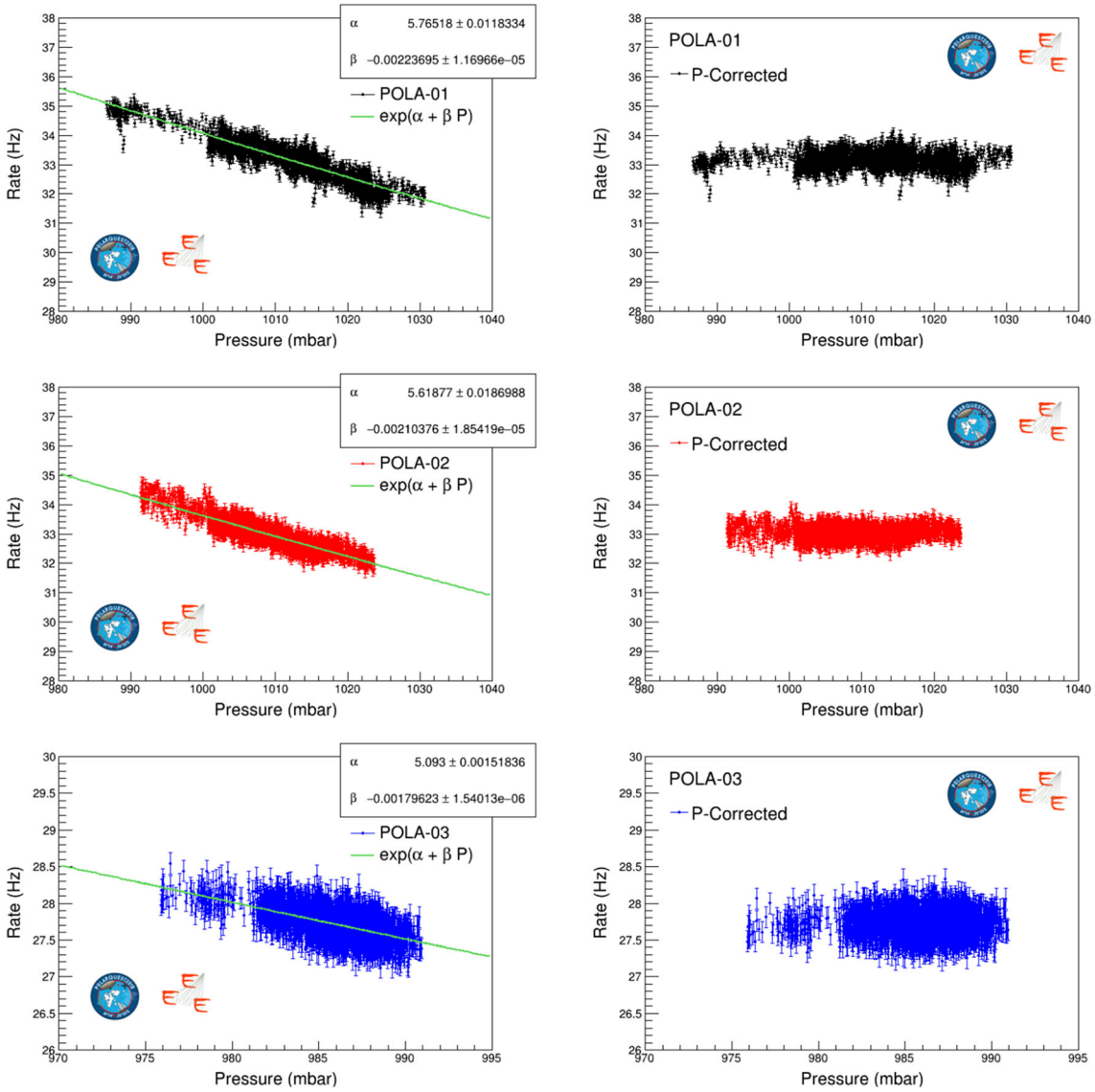


Fig. 22 POLA-01 (top), POLA-02 (middle) and POLA-03 (bottom) rates as a function of the pressure. Left column: rates corrected for the angle with respect to the vertical direction for POLA-01 and raw rate for POLA-02 and POLA-03 (the green line shows the best fit result); right column: rates corrected for the barometric effect at the reference pressure value (see text). Note that the scale used for POLA-03 is reduced with respect to the others

an effect is more evident correspond to strong cross wind, when the boat was sailing with the wind on its side, thus maintaining a constant inclination for hours or even days. After correction, the rate presents a smoother behaviour as a function of time.

5.2 Correction for atmospheric pressure

A correction to the measured raw rates of all three telescopes, related to the variation in rate associated to atmospheric pressure changes, has also to be applied. An increase in pressure, in fact, produces a reduction of the observed rate because the pressure reflects the amount of air that the secondary particles produced by the interaction of primary cosmic rays high up in the atmosphere have to traverse before being detected. This effect has been well known for a long time [32,33].

The raw rate measured by POLA-01 corrected for the inclination effect and the raw rates measured by POLA-02 and POLA-03 are shown vs. pressure in the left panels of Fig. 22. Here each data point represents a run, pressure is the average pressure during that run, and data refer to the whole period of data taking. POLA-03 experienced, during operation, smaller pressure excursions, roughly between 975 and

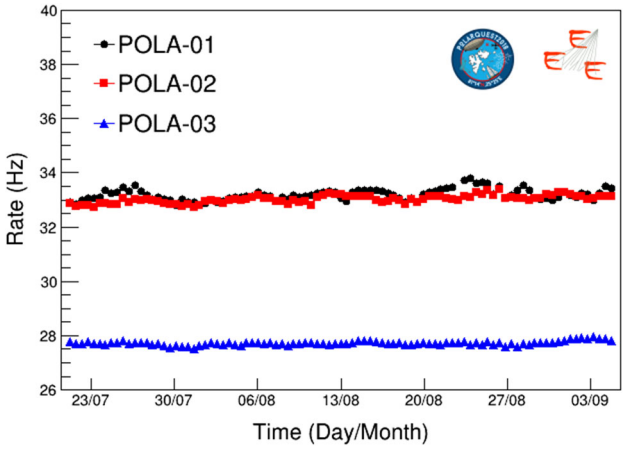


Fig. 23 Rates of cosmic particles measured by the three POLA detectors, corrected for the orientation (POLA-01) and pressure (POLA-01, POLA-02 and POLA-03) effects, as a function time since July 22, 2018

990 mbar, with respect to POLA-01 and POLA-02, both in the 990÷1030 mbar range.

In order to compute the relative correction to the raw data, the data points reported in Fig. 22 were fitted with an exponential law and the relative best fit coefficients, in the following labelled as α and β, were determined for each POLA detector. They are reported in the same Fig. 22.

The barometric correction coefficients $\gamma(p)$, one for each telescope, to the raw rates were computed as: $\gamma = exp[\alpha + \beta(p - p_{ref})]$, where p_{ref} is an arbitrary reference pressure. The average pressures measured by the POLA detectors during the whole data taking were used as p_{ref}; in this way no arbitrary offset to the average corrected rate with respect to the average raw rate is introduced. Reference pressures were 1011.85 mbar for POLA-01, 1008.53 and 985.87 mbar for POLA-02 and POLA-03, respectively. The raw rates were multiplied by $\gamma(p)$ to obtain the corrected rate; p is the average rate measured during a certain run.

Note that, while for POLA-01 and POLA-02 the best fit and barometric coefficients were found to be very similar to each other, POLA-03 appears to be less sensitive to the pressure effect. The difference is probably due the different materials thickness on top the telescopes. In fact, higher material absorption selects higher energetic particles, whose probability to be absorbed in air is lower.

The rates corrected following the procedure described above are shown in the right panels of Fig. 22 and indeed no dependence on the rate with pressure can be observed any more. It has also been verified that the results do not significantly change if the pressure correction is performed using, in place of the average pressure during a certain run, the average pressure measured during 1, or 5, or 10 min time slots, and the relative raw rates.

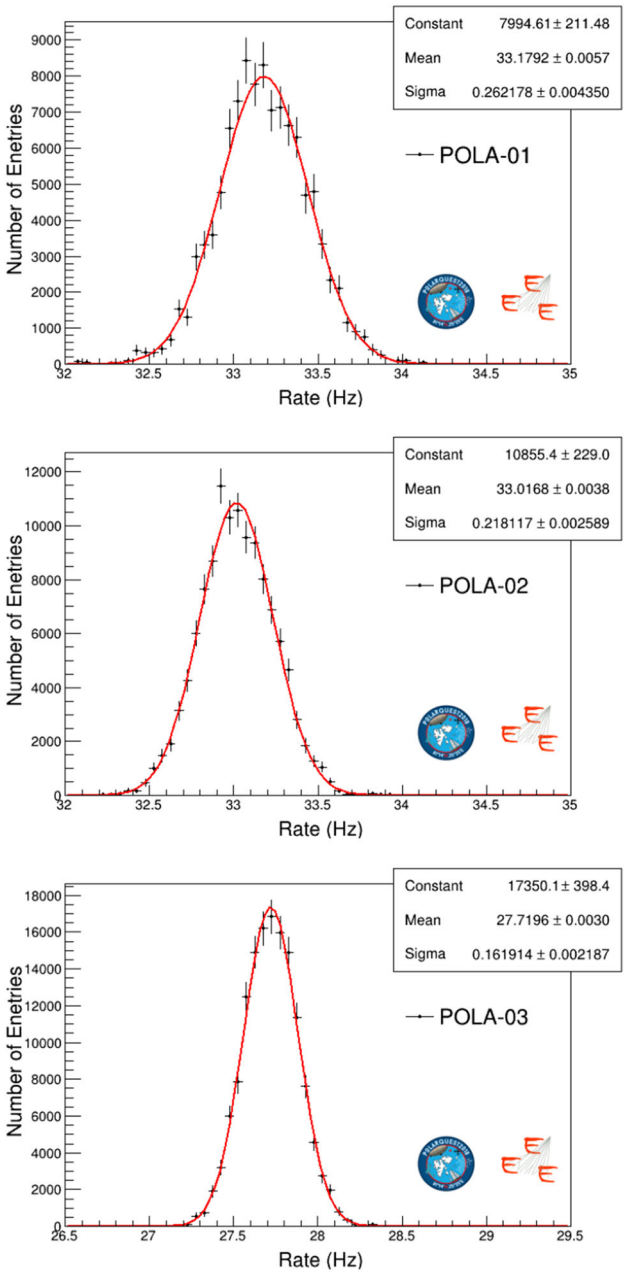


Fig. 24 Distributions of the rate observed by the three POLA detectors during data taking, with Gaussian fits superimposed

Note that the absolute values of the raw rates measured with the POLA detectors are also affected by other effects, like, for instance, the different latitudes they were located at, and their altitude with respect to the sea level. These effects are expected to be more relevant for POLA-03, which was much Southern located than the others, and on a low hill. In this case, roughly, they should amount to some percent. However, since the main goal of this analysis was to determine a possible dependence of the rate measured by POLA-01 on latitude during its trip in the Arctic Sea, and since these par-

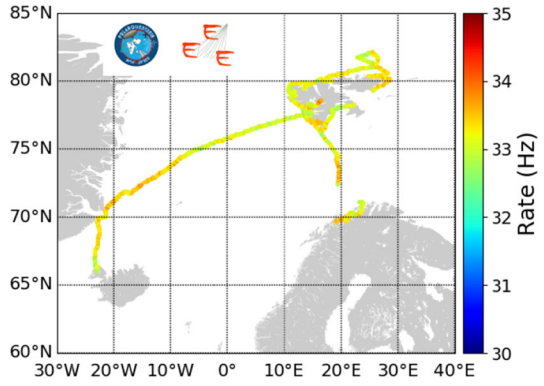


Fig. 25 Rate of cosmic particles, corrected for all the effects mentioned in the previous Section, measured by POLA-01 during its trip in the Arctic Sea

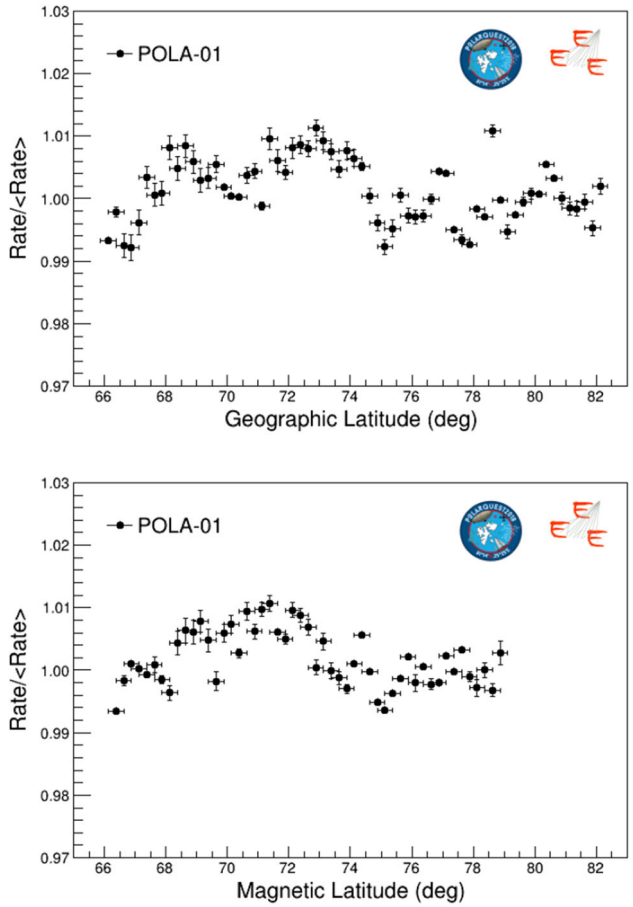


Fig. 26 Top: Rate measured by POLA-01 vs. geographical latitude, divided by the average rate. Bottom: Rate measured by POLA-01 vs. geomagnetic latitude, divided by the average rate

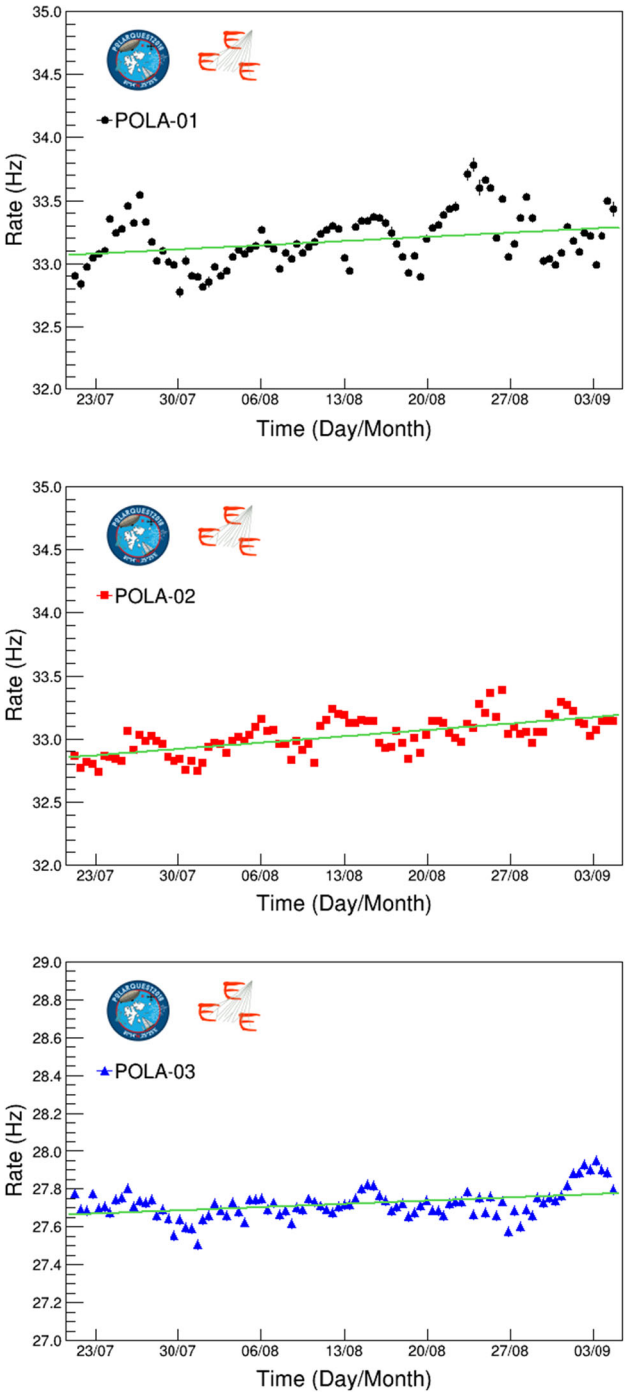


Fig. 27 Cosmic particle rates measured by the POLA detectors as a function of time since July 22, 2018. The green line shows the results of the best fit with a linear function of the time. Note that the scale used for POLA-03 is smaller with respect to the others, to make visible the observed drift

ticular effects do not depend on time or POLA-01 latitude, they do not need to be corrected for.

6 Results

The rates of cosmic particles measured by POLA-01, POLA-02 and POLA-03 during the official data taking period of the

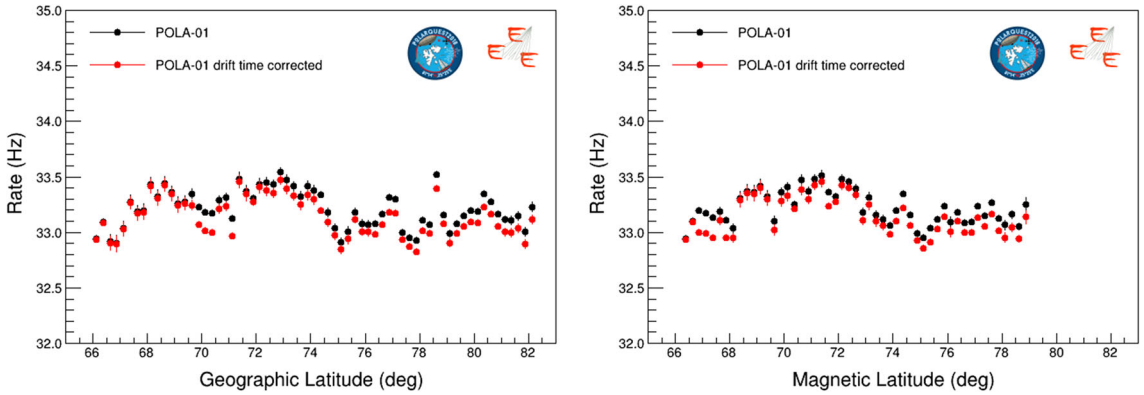


Fig. 28 Rate measured by POLA-01 as a function geographic (left) and magnetic (right) latitude, before (black points) and after long term drift correction (red points)

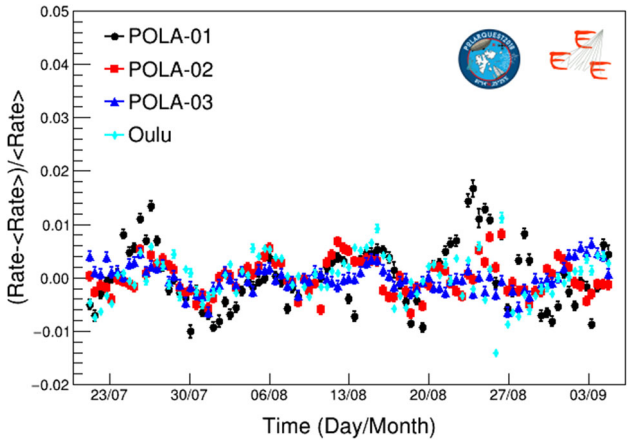


Fig. 29 Percentage rate fluctuations with respect to the average rate measured by the three POLA detectors and by the Oulu neutron monitor, the latter being located at the Sodankylä Geophysical Observatory of the University of Oulu, in Finland, as a function of time

PolarqueEEEst mission, corrected for the pressure and inclination effects described in the previous section, and henceforth here simply called "rate", are reported in Fig. 23 as a function of time. No other correction, for instance due either to the thickness of the materials above the detectors, or their different altitudes, or their efficiency, was applied.

Variations of the rate around their average values are clearly reduced with respect to the ones shown in Fig. 15, in particular for POLA-01 and POLA-02, where they were more evident. Rates stay around an average value of 33.18 Hz for POLA-01, 33.03 Hz for POLA-02 and 27.73 Hz for POLA-03, with small fluctuations with respect to these values. In order to have a quantitative estimate of such fluctuations, histograms of the observed rates were done, and the relative distributions fitted with Gaussians. They are shown in Fig. 24, and demonstrate that they are around 0.26 Hz, 0.22 Hz and 0.16 Hz for POLA-01, POLA-02 and POLA-03, respectively, namely $< 1\%$.

The map of the trip marked with the rate measured by POLA-01 (corrected for the effects mentioned above), is reported in Fig. 25. The zones shown in Fig. 17 where, apparently, the rate significantly deviated from its average value, are not visible anymore.

In order to more easily recognize a possible correlation of the rate measured by POLA-01 with the latitude where the detector was located, the rate as a function of latitude, divided by the average rate, is shown in Fig. 26-top. For each data point here the measured rates have been averaged across all data taken at a certain geographic latitude, regardless of the time of data taking, and the errors reported on the rate are statistical. The rate measured by POLA-01 stays more or less constant around its average value, with fluctuations generally contained in the $\pm 1\%$ band around it, as already said. Apparently, no clear trend can be seen, which could suggest a possible dependence of the measured cosmic particle rate on the latitude.

The rate measured by POLA-01 divided by its average value, as a function of the geomagnetic latitude, is also shown in Fig. 26-bottom. Indeed, in the very northern regions, geographical and geomagnetic latitudes can significantly differ, and this is confirmed, for instance, by the fact that the northernmost geomagnetic latitude reached by the Nanuq was less than 80° N, to be compared with the 82° N of geographic latitude. Nevertheless, no clear evidence of any trend of the rate vs. geomagnetic latitude is visible in Fig. 26.

In order to understand the origin of the observed ± 1 % fluctuations around the average value of the cosmic particle rate measured by POLA-01, a comparison with the rates measured by POLA-02 and POLA-03 is useful. In fact, if some external cause would affect the primary cosmic ray flux, like, for instance, small changes in the Solar activity, night-day variations, seasonal modulations, or else, this should affect the measurements performed with all three detectors.

Indeed some common behaviour can be observed by studying the cosmic particle rates measured by the three

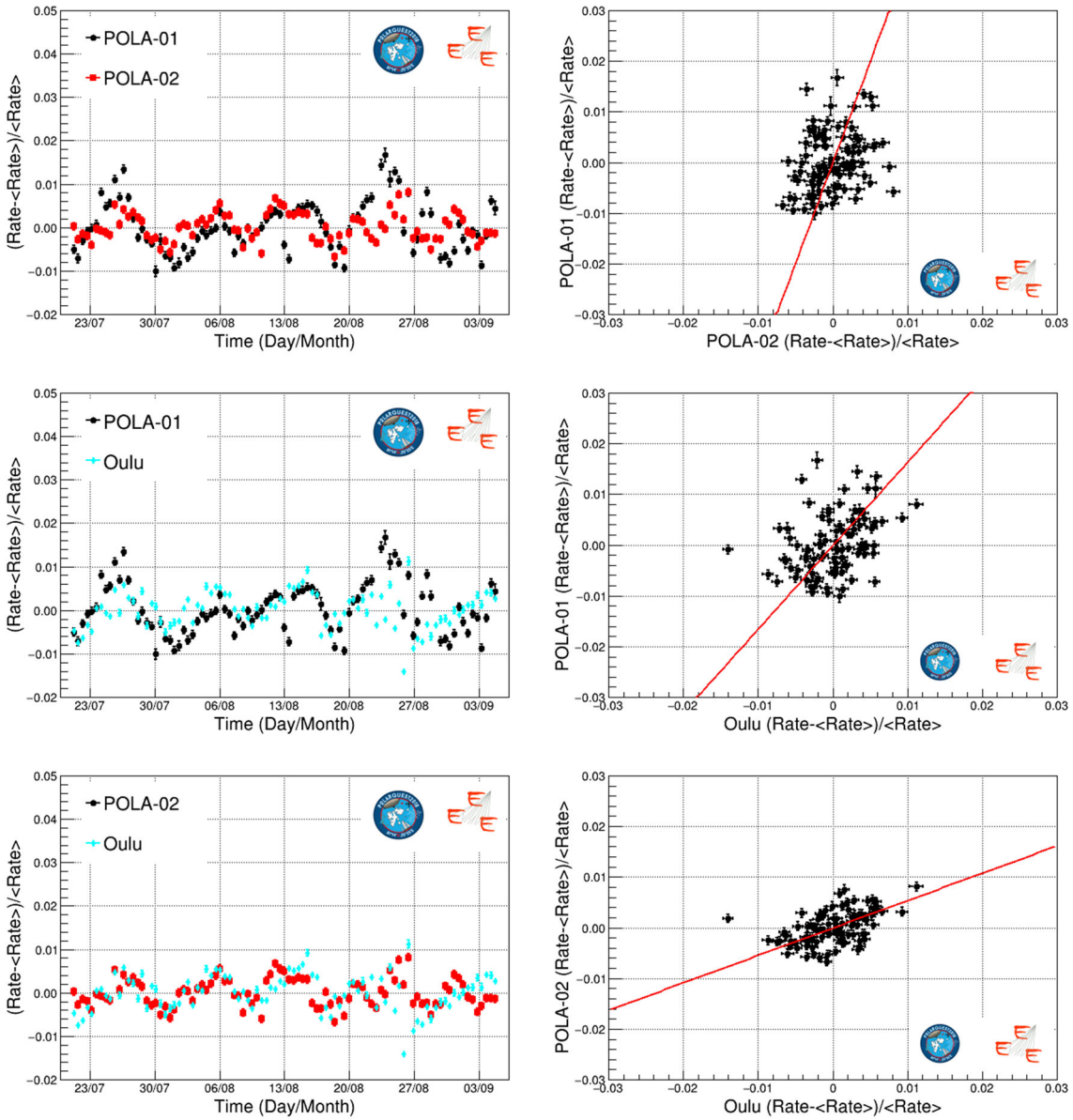


Fig. 30 Percentage rate variations as a function of the time (left column) and rate variation correlation plot (right column). Top row: POLA-01 and POLA-02; middle row: POLA-01 and Oulu; bottom row: POLA-02 and Oulu. The red line shows the fit with a linear function. The correlation coefficients from the top to the bottom are 0.31, 0.35 and 0.50, corresponding to p-values of 2.8×10^{-3}, 6.8×10^{-4} and $< 10^{-5}$, respectively

POLA detectors during data taking. In particular, one common behaviour is a time drift of the average rates. Rates measured by POLA-01, POLA-02 and POLA-03 are shown in Fig. 27, where it is evident that all three detectors measured an increase of the rate of the order of a few tenths of percent over a time interval of about six weeks, which can therefore be attributed to a common external cause.[2]

To take into account this effect, a linear fit has been performed, as shown in Fig. 27, and the baseline corresponding to the best fit has been subtracted to the measured rate values. Thereafter, a direct comparison between the cosmic particle percentage rate fluctuations measured by the various detectors can be done.

The rate measured by POLA-01 during its whole trip on the sailboat Nanuq is shown in Fig. 28 as a function of geographic latitude, precisely from 62°07′ N to 82°07′ N, before and after correcting for the time drift effect pointed out in

[2] This rate variation, further measured with one of the POLA detectors on ground over a much longer period of time (nearly one year long), appears to be season dependent and is currently under investigation.

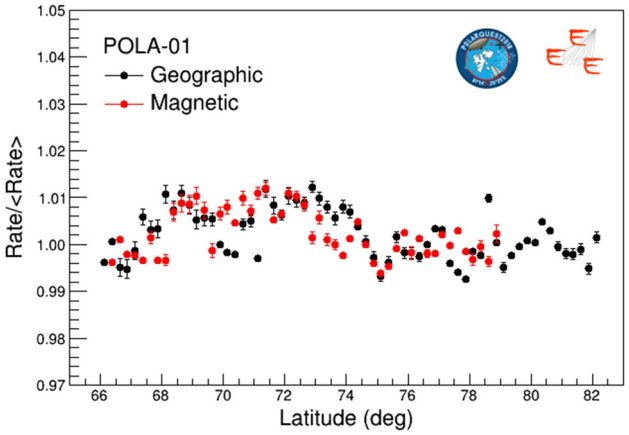


Fig. 31 Rate measured by POLA-01, divided by the average rate, as a function of geographic (black points) and geomagnetic (red points) latitude, once all corrections have been applied. All data points fall within a ±1% band around the average

Fig. 27. Indeed, during its trip, Nanuq passed twice at certain latitudes, a few weeks after having performed the first measurements, and this resulted in a slightly different measured rate. In the same Fig. 28 the same rate is also shown as a function of geomagnetic latitude.

Rate percentage variations with respect to the average rates vs. time have been computed after the drift subtraction for POLA-01, POLA-02 and POLA-03, and are shown all together in Fig. 29. Also the rate fluctuations of the cosmic neutrons measured by a detector of the Global Neutron Network, located at the Sodankylä Geophysical Observatory of the University of Oulu, in Finland [34], at 67°22′ N, 26°38′ E, 180 m altitude, are shown in the same Figure. Indeed, a very similar behaviour in the rate fluctuations measured by the three POLA detectors around their central value can be clearly observed, with oscillations synchronized in time and roughly equal in amplitude and direction.

This is also evident in the first row of Fig. 30-left, where the percentage rate variations with respect to the average rate measured by the closest POLA detectors, namely POLA-01 and POLA-02, are shown. Here, in particular during the first weeks of data taking, oscillations with a roughly weekly period are visible, measured in both detectors. In the same Fig. 30-right, a correlation plot between the rate percentage fluctuations measured by the two POLA detectors at the same time is shown, featuring a correlation coefficient of 0.51, corresponding, given the total number of 91 data points used, to a p-value of 2.8×10^{-3}.

A similar comparison is shown in the second row of the same Fig. 30, obtained this time using POLA-01 data and the rate of the cosmic neutrons measured by the neutron detector located at Oulu. Also a comparison between POLA-02 and Oulu is shown in the third row of the same Fig. 30. Correlations coefficients for these two plots are, respectively, 0.35 and 0.5, corresponding to p-values of 6.8×10^{-4} and $< 10^{-5}$.

It can be noticed that POLA-01 rate, measured on board of Nanuq, is affected by somehow larger fluctuations with respect to the ones measured by POLA-02 or at Oulu, as can also be inferred from Fig. 30. However, the fact that the same weekly oscillations in the rate of cosmic particles are simultaneously observed in detectors which are: i) far from each other, ii) operated in different conditions; iii) sensitive to different kinds of particles (namely mainly muons vs. neutrons), is a strong hint that these are of common origin and not related with POLA-01 location or latitude. They can likely be attributed to some kind of Solar cosmic ray modulation, and this aspect is worth to be investigated further.

Finally, Fig. 31 summarizes the results, showing the cosmic particle rate, divided by the average rate, vs. latitude measured by POLA-01 on board of the sailboat Nanuq, once all corrections have been applied, including the latter for time drift. A uniform behaviour is found within an unprecedented precision of ±1%.

7 Conclusions

The PolarquEEEst experiment, installed on the sailing boat Nanuq, has carefully measured the cosmic particle rate at sea level in the extreme northern latitude interval 66° ÷ 82° N, where no accurate and systematic measurements were available. The measured cosmic rate, after corrections, does not show any evidence of dependence on either the geographic or geomagnetic latitude where it was measured, thus indicating a constant cosmic ray flux in the latitude range considered, within a ±1% accuracy. This result, obtained at sea level in an almost unmeasured region well beyond the Arctic Circle, confirms the trend already observed almost one century ago, in the 1930s, and is consistent with the effects of the Earth magnetic field near the North Pole.

In order to understand the origin of the residual fluctuations in the measured rate, not correlated with latitude, data have also been analyzed in conjunction with the ones of two twin reference detectors installed inside two high schools in Nesodden (Norway) and Bra (Italy) and of an additional cosmic neutron detector located at Oulu (Finland). Many of the observed features in the rates are common, leading to the conclusion that they are actually due to a common external cause.

After the Polarquest2018 mission, one of the PolarquEEEst detectors (POLA-01) was used to take data on cosmic rays in a tour on the road along the Italian peninsula and thereafter in Germany and Switzerland, with the aim to obtain a complete scan, with the same detector, of the cosmic particle rate over a wider latitude interval. The results obtained will be presented in a forthcoming paper.

Acknowledgements We thank for the strong support P. Catapano, leader of the Polarquest2018 naval expedition, P. Gallinelli, designer and skipper of Nanuq, and M. Struik, L. Machet and A. Rolandi and the whole crew for their help during the voyage with POLA-01. We thank the students and teachers of the Nesodden Videregående Skole and of the Liceo "Giolitti-Gandino" in Bra for hosting POLA-02 and POLA-03, and all students and teachers who took part in the construction of the POLA detectors at CERN in May 2018. We thank the personnel of the CNAF and ReCaS, the data centers where data of the EEE and PolarquEEEst experiments were stored for subsequent analysis. We also warmly thank the designers and operators of the Oulu Neutron Monitor detector and the Sodankylä Geophysical Observatory, whose data were used in this paper. M.Battaglieri is supported by the U.S. Department of Energy, Office of Science, Office of Nuclear Physics, under contract DE-AC05-06OR23177

Data Availability Statement This manuscript has associated data in a data repository. [Authors' comment: Data are freely available at the EEE monitor website: https://eee.centrofermi.it/monitor/.]

Open Access This article is licensed under a Creative Commons Attribution 4.0 International License, which permits use, sharing, adaptation, distribution and reproduction in any medium or format, as long as you give appropriate credit to the original author(s) and the source, provide a link to the Creative Commons licence, and indicate if changes were made. The images or other third party material in this article are included in the article's Creative Commons licence, unless indicated otherwise in a credit line to the material. If material is not included in the article's Creative Commons licence and your intended use is not permitted by statutory regulation or exceeds the permitted use, you will need to obtain permission directly from the copyright holder. To view a copy of this licence, visit http://creativecommons.org/licenses/by/4.0/.
Funded by SCOAP[3].

References

1. L. Dorman, *Cosmic Rays in Magnetospheres of the Earth and other Planets*, vol. 358 (Springer Science & Business Media, New York, 2009)
2. Arthur H. Compton, A geographic study of cosmic rays. Phys. Rev. **43**, 387–403 (1933)
3. G. Lemaître, M.S. Vallarta, On Compton's Latitude Effect, of Cosmic Radiation. Phys. Rev., 43:87–91, Note that on the original Compton's paper, this article is incorrectly referred to as. Phys. Rev. **42**(917), 1932 (1933)
4. http://www.polarquest2018.org
5. František Běhounek, Atmospheric-electric researches made in 1928 during the Nobile Arctic Expedition in collaboration with Professor A. Pontremoli (Milan) and Professor F. Malmgren (Upsala). *Terrestrial Magnetism and Atmospheric Electricity*, 34(3), 173–198, (1929)
6. G. Casagrande, The historical site of Virgohamna and Andrée's and Wellman's Arctic expeditions. Remarks based on an expeditive survey by drones. submitted to Bollettino della Società Geografica Italiana
7. R. Nania, O. Pinazza, Measuring cosmic ray showers near the North Pole with the Extreme Energy Events project. Il Nuovo Saggiatore **34**(5–6), 27 (2018)
8. https://eee.centrofermi.it/
9. Antonino Zichichi, *Extreme Energy Events - La Scienza nelle Scuole* (Società Italiana di Fisica, Bologna, 2017)
10. M. Abbrescia et al., (EEE collaboration). The Extreme Energy Events experiment: an overview of the telescopes performance. JINST, 13(08), P08026, (2018)
11. M. Abbrescia et al., (EEE collaboration). Observation of the February 2011 Forbush decrease by the EEE telescopes. Eur. Phys. J. Plus, **126**, 61, (2011)
12. M. Abbrescia et al., (EEE collaboration). Looking at the sub-TeV sky with cosmic muons detected in the EEE MRPC telescopes. Eur. Phys. J. Plus, **130**, 187, (2015)
13. M. Abbrescia et al., (EEE collaboration). Time Correlation measurements from extensive air showers detected by the EEE telescopes. Eur. Phys. J. Plus, **128**, 148, (2013)
14. M. Abbrescia et al., (EEE collaboration). Search for long distance correlations between extensive air showers detected by the EEE network. Eur. Phys. J. Plus, **133**, 34, (2018)
15. https://www.intel.it/content/www/it/it/products/programmable/fpga/cyclone-v.html
16. J. Christiansen, HPTDC High Performance Time to Digital Converter. Technical report, CERN, Geneva, Version 2.2 for HPTDC version 1.3 (2004)
17. https://www.ftdichip.com/Products/ICs/FT232H.htm
18. https://www.u-blox.com/en/product/evk-m8xzoe
19. http://www.cqrobot.wiki/index.php/Raspberry_Pi_GPS_Module_kit-CQR0048
20. https://www.raspberrypi.org/products/raspberry-pi-3-model-b-plus/
21. https://www.maximintegrated.com/en/products/sensors/DS18B20.html
22. https://www.adafruit.com/product/381
23. https://astro-pi.org/
24. https://www.st.com/en/mems-and-sensors/lsm9ds1.html
25. https://www.st.com/en/mems-and-sensors/lps25h.html
26. https://www.st.com/en/mems-and-sensors/hts221.html
27. https://www.adafruit.com/product/2652
28. https://www.bosch-sensortec.com/bst/products/all_products/bme280
29. https://www.bosch-sensortec.com/bst/products/all_products/bno055
30. https://eee.centrofermi.it/monitor/
31. S. Pethuraj et al., Measurement of Cosmic Muon angular distribution and vertical integrated flux by 2 m × 2 m RPC stack at IICHEP-Madurai. JCAP **09**(21), (2017)
32. L. Myssowsky, L. Tuwim, Unregelmassige Intensitätsschwankungen der Hohenstrahlung in geringer Seehohe. Zeitschrift fur Physik A Hadrons and Nuclei **39**(2–3), 146–150 (1926)
33. E. Steinke, Wasserversenkmessungen der durchdringenden Hesschen Strahlung. Zeitschrift fur Physik A Hadrons and Nuclei **58**(3–5), 183–193 (1929)
34. https://cosmicrays.oulu.fi/